International Journal of Microwave and Wireless Technologies

cambridge.org/mrf

Compact wideband circularly polarized planar monopole antenna for integrated wireless applications

Susmita Bala[1], Biplab Bag[2], Sushanta Sarkar[3] and Partha Pratim Sarkar[3]

[1]Department of Electronics, Vidyasagar University, Midnapore, WB, India; [2]Department of Electronics and Communication Engineering, Haldia Institute of Technology, Haldia, WB, India and [3]Department of Engineering and Technological Studies, University of Kalyani, Kalyani, WB, India

Research Paper

Cite this article: Bala S, Bag B, Sarkar S, Sarkar PP (2025) Compact wideband circularly polarized planar monopole antenna for integrated wireless applications. *International Journal of Microwave and Wireless Technologies* **17**(8), 1400–1408. https://doi.org/10.1017/S175907872510264X

Received: 12 June 2025
Revised: 11 November 2025
Accepted: 19 November 2025

Keywords:
circular polarization; modified C-shaped; planar monopole antenna; wideband

Corresponding author: Susmita Bala;
Email: susmitabala@mail.vidyasagar.ac.in

Abstract

This work proposes a small, wideband circularly polarized planar monopole antenna. The antenna comprises a modified C-shaped radiating patch and a truncated rectangular ground plane with a small open-ended slot to achieve a wideband circular polarization property. The proposed antenna has a compact volume of $0.57\lambda_0 \times 0.45\lambda_0 \times 0.024\lambda_0$ (where λ_0 is the free space wavelength at resonant frequency of 4.5 GHz). It provides a measured fractional impedance bandwidth of 50.70% and fractional 3 dB axial ratio bandwidth of 45.04%. The measured peak gain of the antenna is 7.4 dBi. It also maintains a gain of more than 6 dBi throughout the entire band. The mechanism of circular polarization is also described herein. A parametric investigation of various design parameters has also been prepared herein. The proposed model was simulated using the High Frequency Structure Simulator, and measurements were conducted to validate the simulated results. The simulated and measured results of the various characteristics of the proposed antenna are presented. Owing to its low-profile, wideband, and circular polarization characteristics, the proposed antenna is applicable for different wireless applications.

Introduction

Microstrip antennas offer a host of compelling advantages, including low profile, compact size, easy integration with electronic devices, cost-effectiveness, and simple fabrication [1]. However, one notable drawback is their narrow bandwidth. To overcome this limitation, various techniques for broadening the bandwidth of microstrip antennas have been extensively explored and reported in prestigious journals. Wideband microstrip antennas are particularly beneficial, as they enable high data rates with low power spectral density [2]. Additionally, these antennas can be made to generate circular polarization (CP) by modifying the radiating patch, adjusting the ground plane, utilizing slot geometry, or incorporating split-ring resonators, etc., as discussed in numerous renowned studies. CP plays a crucial role in reducing multi-path effects and eliminating antenna orientation restrictions [3]. This section has documented a variety of antenna types with various patch shapes, feed lines, slots, etc., that can significantly provide high gain, wideband, and CP characteristics. L-like strip and hook-like ground plane were used for wideband CP. A hook-shaped microstrip antenna for CP operation was reported in [4]. CP was achieved by using monopole geometry with parasitic strips in [5]. L-shaped monopole antenna and falcate-like monopole antenna were reported for CP characteristics in [6, 7]. By using a modified ground plane, CPs were achieved in two cases [8, 9]. A C-like monopole with a modified feed line was responsible for 37.1% of axial ratio bandwidth (ARBW) in [10]. A trapezoidal antenna provides 36% ARBW was published in [11]. About 52% of ARBW has been achieved in [12]. A monopole antenna was proposed for 2.38–4.60 GHz ARBW in [13]. 18.6% of ARBW was achieved in [14]. The C-shaped slit was responsible for CP operations were informed in [15]. An ultrawideband antenna was responsible for CP operation in [16]. An antenna with CP operation was made up of a modified ground plane was published in [17, 18]. The CP antenna is composed of a falcate-shaped monopole that has achieved an AR bandwidth of 94% in [19]. An ARBW of approximately 13.67% was informed for a T-like monopole antenna in [20]. Simple monopole geometry provides CP operations for different wireless applications in [21]. A coplanar waveguide-fed CP antenna with 62.6% ARBW was proposed in [22]. Parasitic loops were used for CP operation for a monopole antenna was informed in [23]. A proposed CP antenna used an inverted T-shaped patch was informed in [24]. A proposed structure consisting of a wide-slotted hexagonal geometry has been proposed for CP operation

© The Author(s), 2025. Published by Cambridge University Press in association with The European Microwave Association.

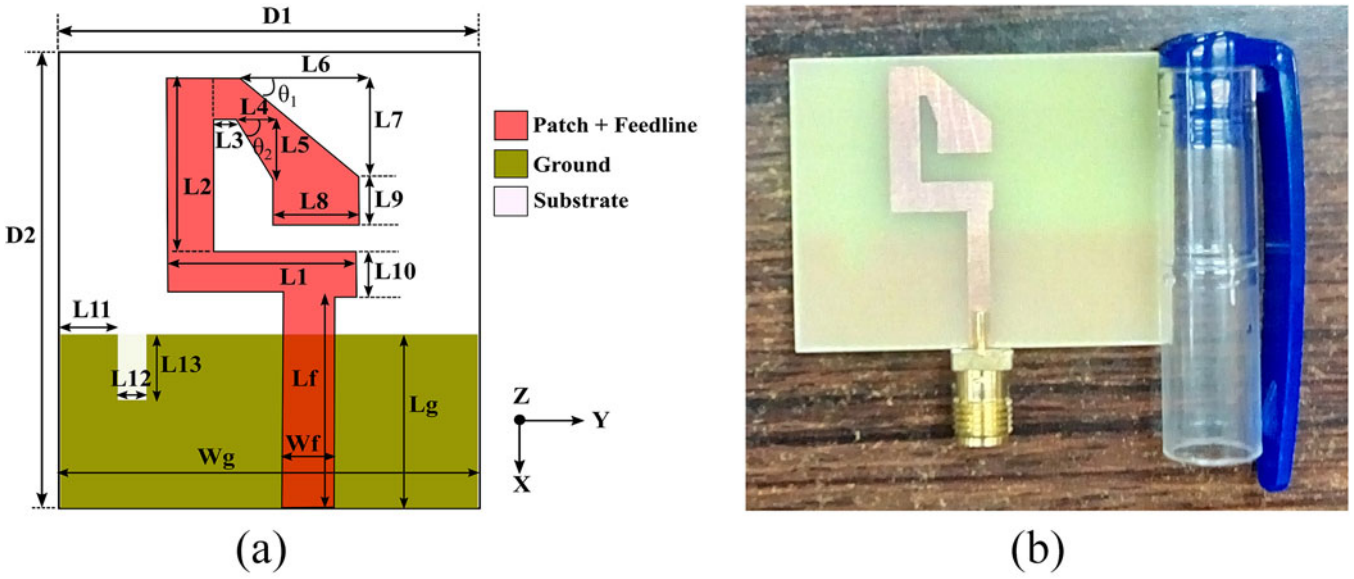


Figure 1. (a) Geometry of the proposed antenna. (b) Fabricated proposed antenna.

Table 1. Dimensions of the proposed antenna (in mm)

D1	D2	Wf	Lf	Wg	Lg	L1
38	30	2.2	14	38	12	10.52
L2	L3	L4	L5	L6	L7	L8
12.06	0.885	1.045	2.82	6.54	5.82	5.53
L9	L10	L11	L12	L13	θ_1	θ_2
3.18	3.06	5	2	4	~42°	~70°

and has been reported in [25]. In total, 102.6%, 62%, and 83.2% of ARBW were proposed for various applications in [26–28]. A wideband CP antenna was proposed for the global satellite navigation system in [29]. A compact antenna provides multiple bands and dual CP for navigation systems in [30]. A microstrip antenna uses dipole fractal geometry was suggested for small satellite applications in [31]. A CP antenna supports GPS L1, L2, and L5 bands were reported in [32]. A small antenna uses fractal patch and slots to obtain the CP operation was proposed for navigation systems in [33]. A wideband suggested antenna useful in satellite and other communication systems was informed in [34]. An investigation of performance on microstrip antennas was done for satellite applications in [35]. Using L-like microstrip feed line, a monopole antenna provides wideband CP in [36]. A Wideband CP antenna array was proposed for CP operation in [37]. A planar monopole CP antenna with simple radiator structure was proposed in [38]. A metasurface-based broadband CP antenna was proposed in [39].

This article reports on a planar simple antenna configuration that produces wideband CP using a modified C-shaped radiating strip and a truncated ground plane. The suggested planar monopole antenna was designed and optimized using the High Frequency Structure Simulator (HFSS). The simulated and experimental findings are compared to ascertain the proposed antenna's correctness. The suggested antenna's wide impedance bandwidth (IBW) (−10 dB) and AR (3 dB) bandwidth are finally obtained by simply scaling the different dimensions of radiating patch and slot of the ground plane. Our proposed work provides simple and easy geometry. It uses a single-layer substrate. Without using any complex geometry, it provides wide −10 dB IBW and 3 dB ARBW. Also, without using any frequency selective substrate, metasurface, array, and stacked substrate, it provides high gain. Due to low profile and above said characteristics, the proposed antenna may be useful in the various wireless systems.

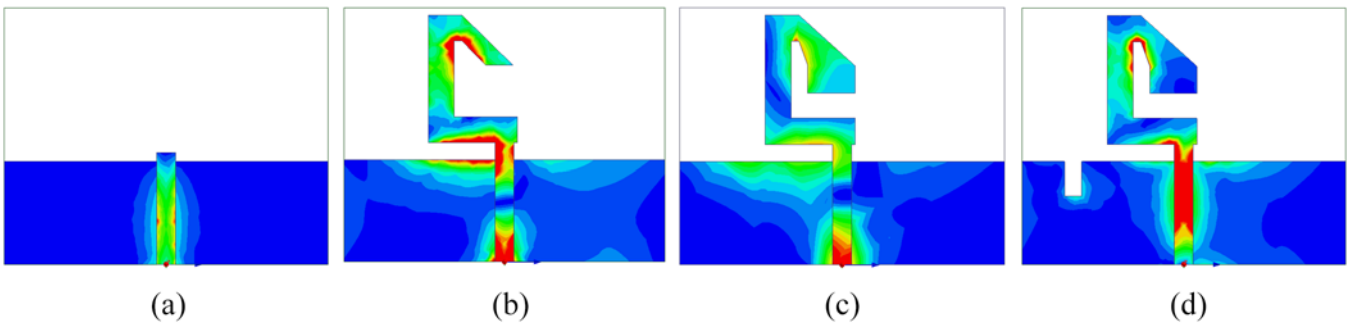


Figure 2. Development steps of the proposed antenna. (a) Antenna1. (b) Antenna2. (c) Antenna3. (d) Antenna4 (proposed antenna).

https://doi.org/10.1017/S175907872510264X Published online by Cambridge University Press

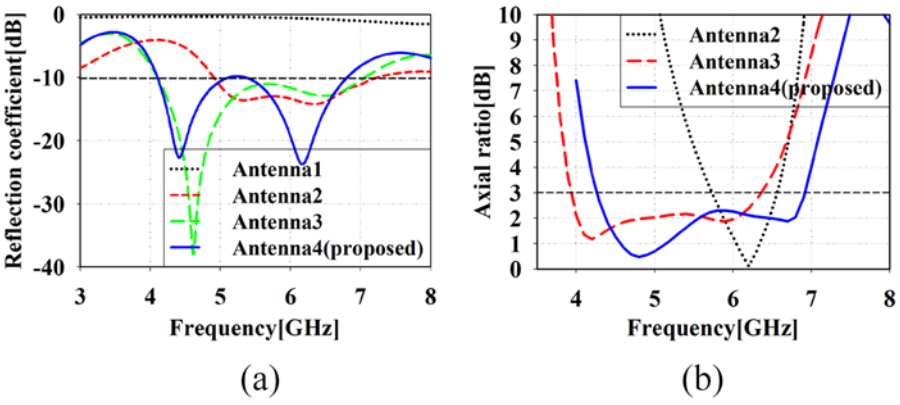


Figure 3. The comparison of the simulated (a) reflection coefficient versus frequency and (b) axial ratio versus frequency for different steps of the proposed antenna.

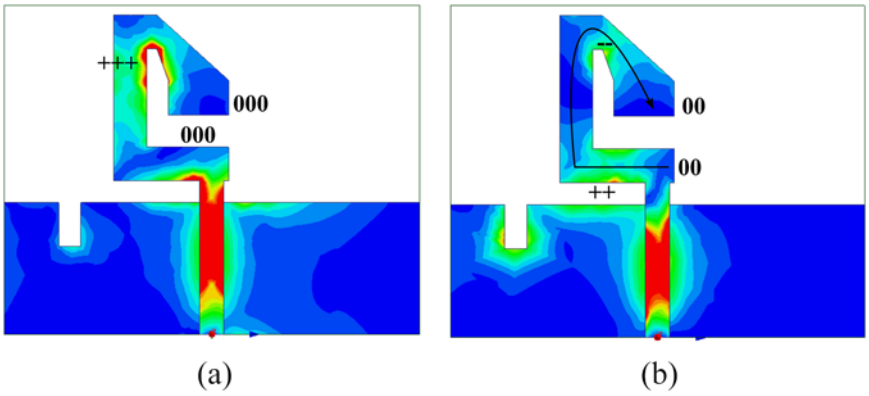


Figure 4. Surface current distribution of the proposed antenna at (a) 4.5 GHz and (b) 6.2 GHz.

Antenna structure

Figure 1(a) depicts the geometry of the proposed antenna structure. The snapshot of the fabricated proposed antenna is shown in Figure 1(b). Software HFSS is used to design the antenna. It comprises a modified C-shaped radiating patch and a partial rectangular ground plane with a narrow open-ended slot. The FR4 dielectric substrate material, with a height (h) of 1.6 mm, a relative permittivity (ε_r) of 4.4, and a loss tangent (tanδ) of 0.023, is used for the design of the proposed antenna. The antenna is excited using the microstrip feed line. Table 1 lists all the proposed antenna's dimensions. The development steps of the proposed antenna (Antenna1 to Antenna4) are depicted in Figure 2. Four steps are designed for the development process (Antenna1 to Antenna4). Antenna1 (Figure 2(a)) is the first step where only the microstrip feed-line has been taken. It does not provide any IBW and any ARBW. A C-like patch is connected to Antenna1 to design Antenna2 in Figure 2(b). Antenna2 provides (4.91–7.23) GHz = 2.32 GHz bandwidth with (5.73–6.55) GHz = 0.820 GHz ARBW. Antenna3 connects a rectangular patch with the slant portion of Antenna2 in Figure 2(c). Antenna3 provides (4.11–7.06) GHz = 2.95 GHz bandwidth with (3.92–6.36) GHz = 2.44 GHz ARBW. Next, to design Antenna4, a tiny open-ended slot is added to the ground plane to improve the ARBW. Figure 2(d) explains Antenna4. Antenna4 provides (4.11–6.80) GHz = 2.69 GHz −10 dB IBW with (4.25–6.92) GHz = 2.67 GHz 3 dB ARBW. The comparison of the simulated reflection coefficient versus frequency and the axial ratio versus frequency of different steps of the proposed antenna is plotted in Figure 3(a) and (b),

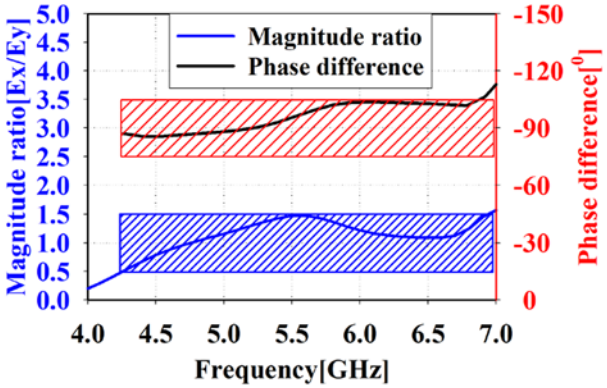


Figure 5. Magnitude ratio and phase difference plot of the proposed antenna.

respectively. After a thorough comparison of the results across all steps, Antenna 4 emerged as the optimal choice, primarily due to its superior ARBW.

Method of design and circular polarization characteristics

In the proposed antenna (Figure 4(a)), the surface current distribution on a C-shaped strip at 4.5 GHz is explored as zero-peak-zero, and the electrical length turns out to be one, where $\frac{\lambda_g}{2}$ is the guided wavelength of the desired resonant frequency. Therefore,

https://doi.org/10.1017/S175907872510264X Published online by Cambridge University Press

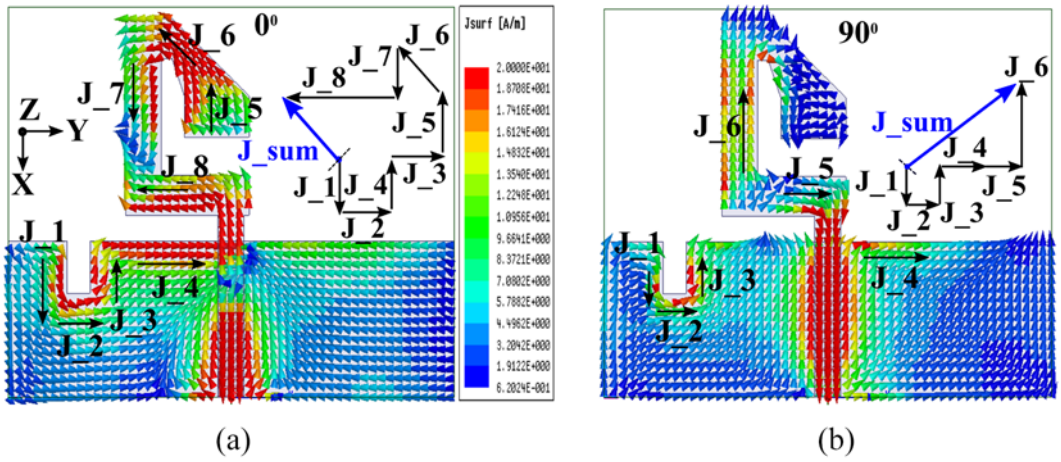


Figure 6. Surface current distribution of the proposed antenna at 4.5 GHz for (a) ωt = 0° and (b) ωt = 90°.

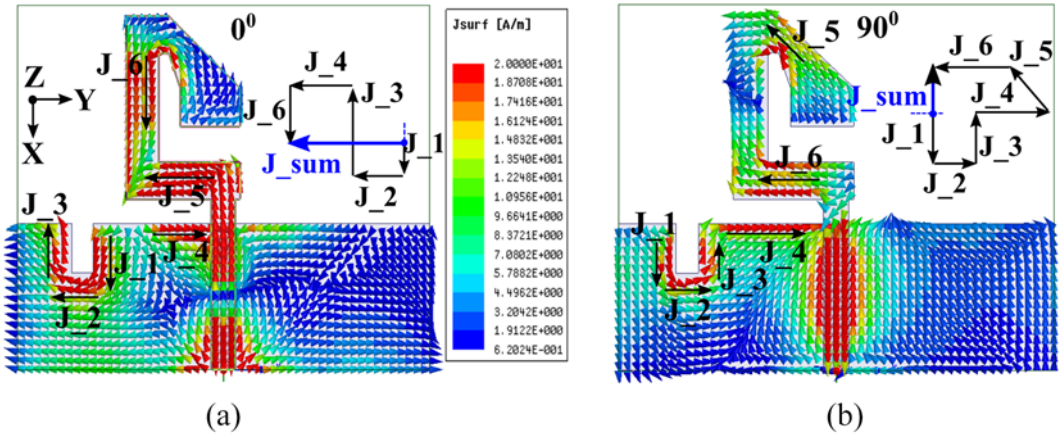


Figure 7. Surface current distribution of the proposed antenna at 6.2 GHz for (a) ωt = 0° and (b) ωt = 90°.

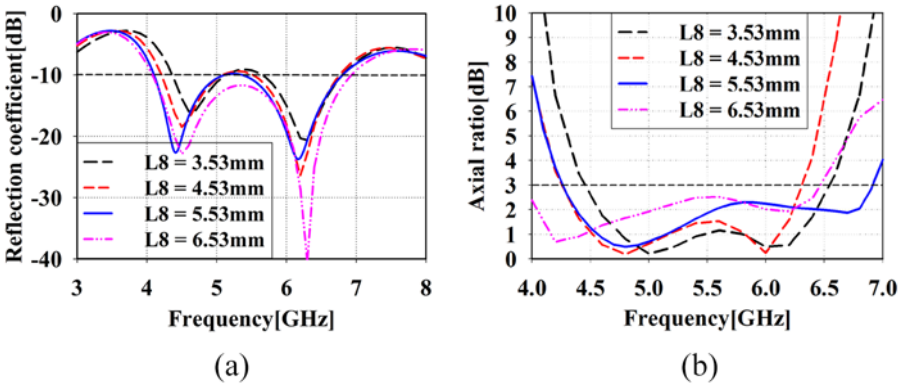


Figure 8. Parametric study for L8 (a) reflection coefficient plot and (b) axial ratio plot.

the length obtained from the current distribution plot (Figure 4(a)) is 22.18 (L2 + L3 + L9 + {$\sqrt{(L4^2 + L5^2)}$+$\sqrt{(L6^2 + L7^2)}$}/2) mm….(i). The dimensions are clearly mentioned in Figure 1 and Table 1, for the above equation (i) and from the reflection coefficient plot (Figure 3(a)), the length is calculated, and it becomes 19.88 mm, which is approximately equal to $\frac{\lambda_g}{2}$. Similarly, in the proposed antenna (Figure 4(b)) at 6.2 GHz, the surface current distribution is assigned as zero-peak-zero-peak, the electrical length turns out to be one guided wavelength (λ_g). Therefore, the length from the current distribution (Figure 4(b)) is 32.71 (L1 + L2 + L3 + L9 + $\sqrt{(L4^2 + L5^2)}$ + $\sqrt{(L6^2 + L7^2)}$) mm and from the reflection coefficient plot (Figure 3(a)) it becomes 29.50 mm (λ_g). Two resonant frequencies (4.5 and 6.2 GHz) are obtained by using equation $f_r = \frac{c}{\lambda_g \sqrt{\frac{\varepsilon_r+1}{2}}}$, where f_r is the resonant frequency, c is the speed of the light and ε_r is the dielectric constant of the substrate. Now, these two resonant frequencies are merged together and produce wide-bandwidth (2.69 GHz).

https://doi.org/10.1017/S175907872510264X Published online by Cambridge University Press

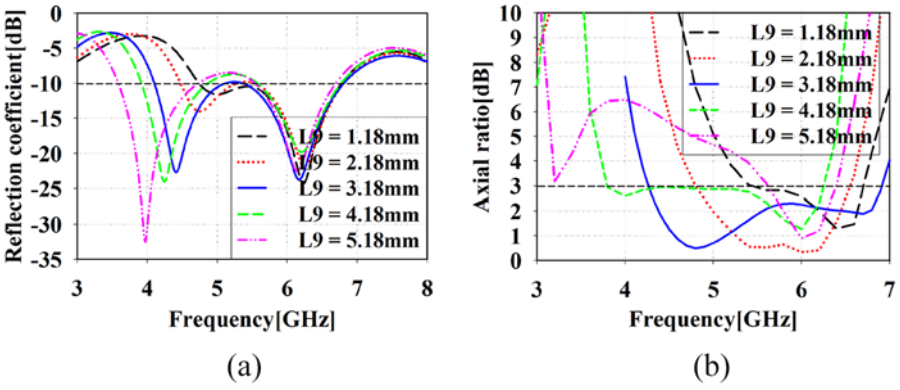


Figure 9. Parametric study for L9 (a) reflection coefficient plot and (b) axial ratio plot.

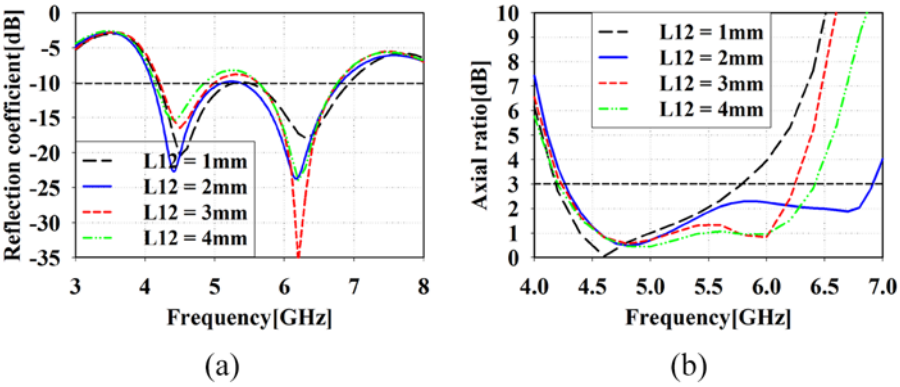


Figure 10. Parametric study for L12 (a) reflection coefficient plot and (b) axial ratio plot.

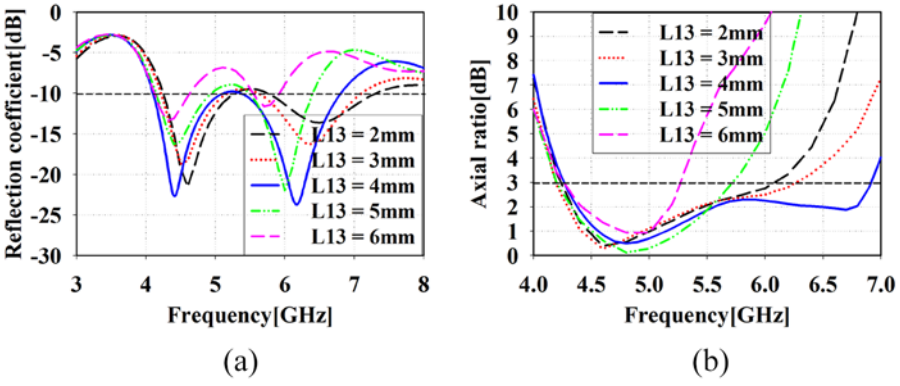


Figure 11. Parametric study for L13 (a) reflection coefficient plot and (b) axial ratio plot.

Table 2. Results of parametric study for L8

Antenna parameter (mm)	Impedance bandwidth (IBW) in GHz	% of IBW	Axial ratio bandwidth (ARBW) in GHz	% of ARBW
L8 = 3.53	(4.4–6.8) = 2.4	42.58	(4.6–6.4) = 1.8	32.72
L8 = 4.53	(4.3–6.8) = 2.5	45.04	(4.4–6.2) = 1.8	33.96
L8 = 5.53	(4.11–6.8) = 2.69	49.31	(4.25–6.92) = 2.67	47.80
L8 = 6.53	(4.1–6.9) = 2.8	50.90	(4–6.4) = 2.4	46.15

Table 3. Results of parametric study for L9

Antenna parameter (mm)	Impedance bandwidth (IBW) in GHz	% of IBW	Axial ratio bandwidth (ARBW) in GHz	% of ARBW
L9 = 1.18	(4.74–6.77) = 2.03	39.96	(5.4–6.6) = 1.2	20
L9 = 42.18	(4.48–6.8) = 2.32	41.13	(4.8–6.4) = 1.6	28.57
L9 = 3.18	(4.11–6.8) = 2.69	49.31	(4.25–6.92) = 2.67	47.80
L9 = 4.18	(3.92–6.77) = 2.85	53.32	(3.8–6.1) = 2.3	46.46
L9 = 5.18	(3.59–6.69) = 3.1	60.31	(5.6–6.4) = 0.8	13.33

https://doi.org/10.1017/S175907872510264X Published online by Cambridge University Press

Table 4. Results of parametric study for L12

Antenna parameter (mm)	Impedance bandwidth (IBW) in GHz	% of IBW	Axial ratio bandwidth (ARBW) in GHz	% of ARBW
L12 = 1	(4.2–6.9) = 2.7	48.64	(4.2–5.6) = 1.4	28.57
L12 = 2	(4.11–6.8) = 2.69	49.31	(4.25–6.92) = 2.67	47.80
L12 = 3	(4.3–4.9) = 0.6 (5.7–6.7) = 1.0	13.04 16.12	(4.4–6.2) = 1.8	33.96
L12 = 4	(4.2–4.8) = 0.6 (5.7–6.7) = 1.0	13.12 16.12	(4.2–6.4) = 2.2	41.50

Table 5. Results of parametric study for L13

Antenna parameter (mm)	Impedance bandwidth (IBW) in GHz	% of IBW	Axial ratio bandwidth (ARBW) in GHz	% of ARBW
L13 = 2	(4.3–7.3) = 3.0	51.72	(4.4–6) = 1.6	30.78
L13 = 3	(4.3–7.1) = 2.8	49.12	(4.2–6.2) = 2.0	
L13 = 4	(4.1–6.8) = 2.69	49.31	(4.25–6.92) = 2.67	47.80
L13 = 5	(4.2–4.9) = 0.7 (5.5–6.3) = 0.8	15.38 13.55	(4.2–5.6) = 1.4	28.57
L13 = 6	(4.2–4.6) = 0.6 (5.6–5.9) = 0.3	13.63 5.21	(4.4–5.2) = 0.8	16.66

Table 6. Comparison between simulated and measured results of the proposed antenna

Parameters	Simulated result	Measured result
Impedance bandwidth (IBW)	2.69 GHz	2.88 GHz
% of impedance bandwidth (% of IBW)	49.31%	50.70%
Axial ratio bandwidth (ARBW)	2.67	2.5
% of axial ratio bandwidth (% of ARBW)	47.80%	45.04%
Peak gain	8.13 dBi at 6 GHz	7.4 dBi at 6 GHz

On the other hand, the proposed antenna exhibits wide CP. For CP, E-field components (Ex and Ey) should have equal in magnitude and ± 90° phase difference between them. These two criteria are graphically shown in Figure 5, where the magnitude is approximately equal to one, and the phase difference is approximately equal to —90° within the operating range. The magnitude ratio and phase difference with respect to frequency of the proposed antenna are shown in Figure 5.

The concept of CP of the proposed antenna at two resonant frequencies (4.5 and 6.2 GHz) is described by using surface current distributions which are shown in Figures 6 and 7. To more the top and ground plane surface current distribution helps to explain the CP mechanism. For that, the surface currents are distributed by

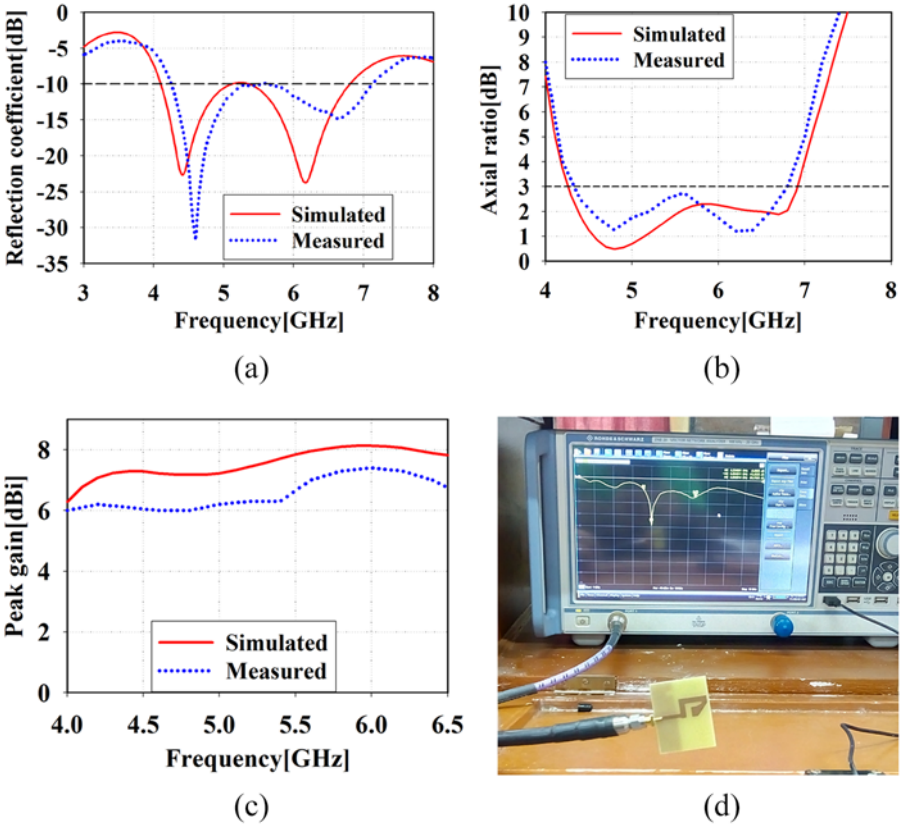


Figure 12. The simulated and measured results of the proposed antenna (a) reflection coefficient versus frequency plot, (b) axial ratio versus frequency plot, (c) gain versus frequency plot, and (d) measurement of the fabricated antenna.

https://doi.org/10.1017/S175907872510264X Published online by Cambridge University Press

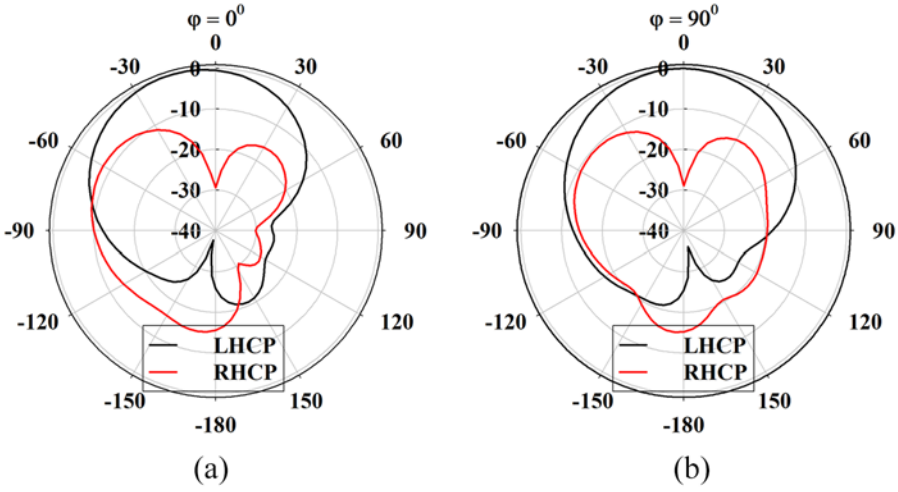


Figure 13. Radiation patterns of the proposed antenna at 4.5 GHz (a) $\varphi = 0°$ and (b) $\varphi = 90°$.

Table 7. Comparison of previous antennas in terms of performance

Ref.	Size in terms of λ_0 at lowest operating frequency of the IBW	−10 dB impedance bandwidth (GHz)	3 dB axial ratio bandwidth (GHz)	Peak gain
[4]	$0.307\lambda_0 \times 0.307\lambda_0 \times 0.0098\lambda_0$	(1.84–2.43) = 0.59	(1.89–2.43) = 0.54	4.60 dBic
[13]	$0.330\lambda_0 \times 0.330\lambda_0 \times 0.012\lambda_0$	(2.25–4.0) = 1.75	(2.38–4.60) = 2.22	3.54 dBic
[15]	$0.487\lambda_0 \times 0.487\lambda_0 \times 0.0327\lambda_0$	(0.859–0.944) = 0.085	(0.902–0.930) = 0.028	5.9 dBic
[33]	$0.3\lambda_0 \times 0.3\lambda_0 \times 0.03\lambda_0$	0.60	(1.57–1.6) = 0.03	3.26 dBic
[36]	$0.342\lambda_0 \times 0.239\lambda_0 \times 0.0109\lambda_0$	(2.05–4.81) = 2.76	(2.3–5.1) = 2.8	4.75 dBi
[37]	$0.95\lambda_0 \times 0.95\lambda_0 \times 0.05\lambda_0$	(4.76–8.3) = 3.54	(5.49–6.29) = 0.8	9.9 dBi
[38]	$0.392\lambda_0 \times 0.473\lambda_0 \times 0.0184\lambda_0$	(3.46–5.5) = 2.04	(3.46–5.5) = 2.04 (6 dB axial ratio BW)	4.3 dBi
[39]	$1.467\lambda_0 \times 1.467\lambda_0 \times 0.055\lambda_0$	(5.5–8.3) = 2.8	(6.3–8.2) = 1.9	5.1 dBic
Proposed work	$0.537\lambda_0 \times 0.424\lambda_0 \times 0.022\lambda_0$	(4.24–7.12) = 2.88	(4.3–6.8) = 2.5	7.4 dBi

the vector components. Figures 6 and 7 illustrate the surface current at 4.5 and 6.2 GHz for two consecutive angular values ($\omega t = 0°$ and $\omega t = 90°$) over one complete rotation of 360°. Therefore, the rotation of the resultant vector sum dictates the orientation [whether it is left-hand circular polarization (LHCP) or right-hand circular polarization (RHCP)] of CP. The resultant surface current (J_sum) consists of the top C-shaped plate and the ground plane. At 4.5 GHz, Figure 6 shows that the resultant vector lies along (−X−Y) direction at $\omega t = 0°$, then it rotates in clockwise direction and directed along (−X+Y) direction at $\omega t = 90°$. Hence, at 4.5 GHz, from the rotation of the resultant surface current, it is concluded that the LHCP wave is produced in + Z direction. Similarly, at 6.2 GHz, Figure 7 shows that the resultant vector lies along (−Y) direction at $\omega t = 0°$, then it rotates in clockwise direction and directed along (−X) direction at $\omega t = 90°$.

Parametric analysis

A thorough parametric study was carried out to assess how antenna dimensions affect CP features and wideband performance. For this research, the key parameters taken into account are L8, L9, L12, and L13. To isolate each parameter's unique influence, HFSS simulations were used to change each one separately while holding the others constant. Figures 8–11 depict the reflection coefficients and axial ratios, while Tables 2–5 provide a summary of the findings, including the IBW, its percentage, and the ARBW and its percentage for every parameter variation.

Influence of L8

Plots of the axial ratio and reflection coefficient for different values of L8 (3.53, 4.53, 5.53, and 6.53 mm) with all other parameters held constant are shown in Figure 8(a) and (b). The IBW continuously improves as L8 increases. On the other hand, the ARBW stays constant for the first two values, maximum at L8 = 5.53 mm, which is 2.67 GHz, and then starts to drop at L8 = 6.53 mm. L8 = 5.53 mm is determined to be the optimal dimension because ARBW is a crucial parameter in this investigation.

Influence of L9

Figure 9(a) and (b) show the performance variations with L9 values ranging from 1.18 to 5.18 mm in 1 mm increments. As L9 increases, a significant improvement in IBW is observed. The ARBW also increases, reaching a maximum at L9 = 3.18 mm, after which it begins to decrease. Based on both the ARBW and the percentage of ARBW, L9 = 3.18 mm is selected as the optimal value for antenna fabrication.

https://doi.org/10.1017/S175907872510264X Published online by Cambridge University Press

Influence of L12

Figure 10(a) depicts that L12 does not significantly affect the IBW for 1 and 2 mm. However, further increases in L12 cause the antenna to exhibit a dual-band characteristic, which is undesirable for this application. Figure 10(b) shows that the maximum ARBW occurs at L12 = 2 mm. So, L12 = 2 mm is considered as optimal value for fabrication.

Influence of L13

The effects of L13 are displayed in Figure 11(a) and (b). For L13 values of 2, 3, and 4 mm, the antenna provides wide IBW. At L13 = 5 and 6 mm, dual-band nature is observed, which is undesirable in this design. Among the five values studied, L13 = 4 mm yields the best IBW and ARBW, making it the final choice for the proposed fabricated design.

After parametric study, the optimal values that are chosen for antenna fabrication are L8 = 5.53 mm, L9 = 3.18 mm, L12 = 2 mm, and L13 = 4 mm.

Result and discussion

The simulated and measured results of the proposed antenna have been discussed here, and the results are tabulated in Table 6. Figure 12(a) presents the reflection coefficient (in dB); illustrating the antenna's simulated IBW ranging from 4.11 to 6.8 GHz, which corresponds to 2.69 GHz IBW with 49.31% of IBW. Figure 12(b) depicts the ARBW ranging from 4.25 to 6.92 GHz, providing a simulated 2.67 GHz ARBW with 47.80% of ARBW. As shown in Figure 12(c), the antenna reaches a peak simulated gain of 8.13 dBi at 6.0 GHz. In case of measurement results, the antenna provides an IBW of 2.88 GHz (4.24 to 7.12 GHz), which is 50.70% of IBW. The measured 3 dB ARBW ranges from 4.3 to 6.8 GHz, resulting in a 2.5 GHz ARBW and 45.04% ARBW. Additionally, a peak measured gain of 7.4 dBi is obtained at 6.0 GHz. Figure 13 depicts the simulated radiation patterns of the proposed antenna at 4.5 GHz for $\varphi = 0°$ and $\varphi = 90°$ planes, providing RHCP and LHCP characteristics.

A comparative study between the proposed work and the studies discussed in the introduction has been done here, providing parameters such as size, bandwidth, 3 dB ARBW, and peak gain. The results of this comparison are presented in Table 7. The results of the comparison indicate that the proposed antenna delivers superior performance compared to the other works discussed.

Conclusion

A C-shaped monopole antenna with a wideband and CP has been introduced in this research study. The antenna consists of a modified C-shaped strip with a small open-ended ground-plane notch. The CP is activated by switching the surface current distribution by interlacing a ground plane and a C-shaped strip. Wide ARBW is achieved by adjusting the ground plane and patch dimensions. The measured fractional bandwidth and ARBW are 50.70% and 45.04%, respectively. The proposed antenna has also produced a measured peak gain of 7.4 dBi. Due to its small size, easy structural design, and wideband CP characteristics, the antenna may be a suitable choice for different wireless communication systems.

Funding statement. This research received no specific grant from any funding agency, commercial or not-for-profit sectors.

Competing interests. The authors report no conflict of interest.

References

1. **Balanis CA** (2005) *Microstrip Antennas in Antenna Theory, Analysis and Design*. USA: John Wiley & Sons, pp. 811–882.
2. **Kumar G and Ray KP** (2003) *"An Introduction to Microstrip Antennas" in Broadband Microstrip Antennas*. USA: Artech House, pp. 1–34.
3. **Bala S** (2024) A single feed circularly polarized dual band microstrip monopole antenna for wireless applications. *Microwave and Optical Technology Letters* **66**. https://doi.org/10.1002/mop.34048.
4. **Samsuzzaman M** (2018) A compact printed monopole antenna with wideband circular polarization. *IEEE Access* **6**, 54713–4725. https://doi.org/10.1109/ACCESS.2018.2871818.
5. **Ding K** (2017) A broadband circularly polarized printed monopole antenna with parasitic strips. *IEEE Antennas and Wireless Propagation Letters* **16**, 2509–2512. https://doi.org/10.1109/LAWP.2017.2728124.
6. **Chandu DS** (2017) A novel broadband dual circularly polarized microstrip-fed Monopole Antenna. *IEEE Transactions on Antennas and Propagation* **65**, 1410–1415. https://doi.org/10.1109/TAP.2016.2647705.
7. **Xu B** (2020) Broadband Circularly Polarized Filtering Monopole Antenna for C-Band Applications. 2020 IEEE International Symposium on Antennas and Propagation and North American Radio Science Meeting, Montreal, QC, Canada
8. **Gyasi KO** (2018) A compact broadband cross-shaped circularly polarized planar Monopole Antenna with a Ground plane extension. *IEEE Antennas and Wireless Propagation Letters* **17**, 335–338.
9. **Lee D, Kim K and Pyo S** (2019) Dual-band monopolar microstrip antenna using a quasi-circularly arranged mushroom resonator on meshed ground structure. *Microwave and Optical Technology Letters* **61**, 1–5. https://doi.org/10.1002/mop.31961.
10. **Kwame OG** (2017) Broadband circularly polarized square slot Antenna with A G-shaped Feedline. IEEE International Symposium on Antennas and Propagation & USNC/URSI National Radio Science Meeting San Diego, CA, USA
11. **Kumar T** (2016) Offset-fed trapezoidal monopole antenna for broadband circular polarization. *International Journal of RF and Microwave Computer-Aided Engineering* **27**. https://doi.org/10.1002/mmce.21063.
12. **Chen Q** (2017) Compact Microstrip-via-fed wideband circularly polarized Antenna with monofilar spiral stub for C-band applications. *International Journal of RF and Microwave Computer-Aided Engineering* **27**. https://doi.org/10.1002/mmce.21118.
13. **Kumar Y** (2018) "Compact broadband circularly polarized hook-shaped Microstrip Antenna with DGS plane. *International Journal of RF and Microwave Computer-Aided Engineering* **28**, e21275. https://doi.org/10.1002/mmce.21275.
14. **Li Z-Y** (2018) A broadband circularly polarized monopole antenna. *International Journal of RF and Microwave Computer-Aided Engineering* **29**. https://doi.org/10.1002/mmce.21687.
15. **Xing Z** (2018) A low-profile aperture coupled antenna with broadband circular polarization characteristics for UHF RFID applications. *International Journal of RF and Microwave Computer-Aided Engineering* **29**. https://doi.org/10.1002/mmce.21688.
16. **Midya M** (2019) Circularly polarized planar monopole Antenna for Ultrawideband Applications. *International Journal of RF and Microwave Computer-Aided Engineering* **29**. https://doi.org/10.1002/mmce.21918
17. **Huang H-F** (2020) A small single fed broadband circularly polarized slot Antenna. *International Journal of RF and Microwave Computer-Aided Engineering* **30**. https://doi.org/10.1002/mmce.22122
18. **Alsariera H** (2020) A compact broadband coplanar waveguide fed circularly polarized printed monopole Antenna with Asymmetric modified ground plane. *International Journal of RF and Microwave Computer-Aided Engineering* **30**. https://doi.org/10.1002/mmce.22205
19. **Xu B** (2020) Broadband circularly polarized printed falcate-shaped monopole antenna. *International Journal of RF and Microwave Computer-Aided Engineering* **30**. https://doi.org/10.1002/mmce.22395

https://doi.org/10.1017/S175907872510264X Published online by Cambridge University Press

20. **Kumar A** (2020) A broadband circularly polarized monopole antenna for millimeter-wave short range 5G wireless communications. *International Journal of RF and Microwave Computer-Aided Engineering* **31**. https://doi.org/10.1002/mmce.22518.
21. **Chandu DS** (2017) Broadband circularly polarized printed monopole Antenna with Protruded L-shaped And Inverted L-shaped Strips. *Microwave and Optical Technology Letters* **60**, 242–248. https://doi.org/10.1002/mop.30953.
22. **Zha H** (2018) A new CPW-fed broadband circularly polarized printed monopole Antenna for UWB Application. *Microwave and Optical Technology Letters* **60**, 364–369. https://doi.org/10.1002/mop.30972.
23. **Feng G** (2019) A broadband circularly polarized monopole antenna employing parasitic loops and defective ground plane. *Microwave and Optical Technology Letters* **62**, 251–256. https://doi.org/10.1002/mop.31998.
24. **Singh K** (2020) A Novel printed circularly polarized asymmetric wide slot antenna for digital cellular system. *Microwave and Optical Technology Letters* **62**, 1438–1447. https://doi.org/10.1002/mop.32177.
25. **Kumar S** (2018) A Low profile circularly polarized UWB Antenna with Integrated GSM Band for Wireless Communication. *International Journal of Electronics and Communications (AEÜ)* **93**, 224–224. https://doi.org/10.1016/j.aeue.2018.06.027.
26. **Zhu Z** (2018) CPW-fed ultra-wideband slot antenna with broadband dual circular polarization. *International Journal of Electronics and Communications (AEÜ)* **98**, 191–198.
27. **Banerjee U** (2019) A CPW-fed compact monopole antenna with defected ground structure and modified parasitic hilbert strip having wideband circular polarization. *International Journal of Electronics and Communications (AEÜ)* **110**, 152831. https://doi.org/10.1016/j.aeue.2019.152831.
28. **Kumar A *et al*** (2020) Wideband circularly polarized parasitic patches loaded coplanar waveguide-fed square slot antenna with grounded strips and slots for wireless communication systems. *International Journal of Electronics and Communications (AEÜ)* **114**, 153011. https://doi.org/10.1016/j.aeue.2019.153011.
29. **Wang L** (2018) a low-profile broadband circularly polarized microstrip antenna with wide beamwidth. *IEEE Antennas and Wireless Propagation Letters* **17**, 1213–1217. https://doi.org/10.1109/LAWP.2018.2839100.
30. **Chen K** (2017) Compact dual-band dual circularly polarized annular-ring patch antenna for BeiDou navigation satellite system application. *IET Microwaves, Antennas & Propagation* **11**, 1079–1085. https://doi.org/10.1049/iet-map.2016.1057.
31. **Simón J** (2017) A microstrip second-iteration square koch dipole antenna for TT&C downlink applications in small satellites. *International Journal of Antennas and Propagation* 1–8. https://doi.org/10.1155/2017/4825179
32. **Mishra S** (2019) Low-profile circularly polarized planar antenna for GPS L1, L2, and L5 bands. *Microwave and Optical Technology Letters* **62**, 1–10.
33. **Wang E** (2022) A compact circular polarized patch fractal antenna for global navigation satellite systems. *Microwave and Optical Technology Letters* **64**, 520–524. https://doi.org/10.1002/mop.33110.
34. **Mukherjee K** (2022) Design of wideband planar antenna with inverted I-shaped tuning stubs for application in 5G, satellite communication, and Internet of Things. *International Journal of Communication Systems* **35**. https://doi.org/10.1002/dac.5240
35. **Mercy PAM** (2024) Novel nanocomposite based microstrip patch antenna for C and X band applications. *Materials Chemistry and Physics* **326**, 129593. https://doi.org/10.1016/j.matchemphys.2024.129593.
36. **Bag B** (2022) Performance enhancement of a circularly polarized printed monopole for wireless system application. *Frequenz, Journal of RF-Engineering and Telecommunications* **76**, 579–592. https://doi.org/10.1515/freq-2021-0230.
37. **Guthi S** (2023) Broadband and high gain circularly polarized mushroom-loaded nonuniform patch array antenna with aperture CPW feed. *Microwave and Optical Technology Letters* **65**, 2565–2571. https://doi.org/10.1002/mop.33737.
38. **Park S** (2024) Design of a circularly polarized planar monopole antenna with a simplified radiator structure for UWB Applications. *Journal of Electromagnetic Engineering and Science* **24**, 145–150. https://doi.org/10.26866/jees.2024.2.r.214.
39. **Ding Z** (2025) Single-layer metasurface-based wideband circularly polarized antenna using CMA with RCS reduction. *International Journal of Antennas and Propagation*. https://doi.org/10.1155/ijap/8836684



Susmita Bala received her M.Tech degree from Jadavpur University, West Bengal, India. She received Ph.D. degree in Engineering from the Department of Engineering and Technological Studies, University of Kalyani in the year 2023. She is currently working as an Assistant Professor at the Department of Electronics, Vidyasagar University. Her research interests include microstrip antenna design for wireless communication systems.



Biplab Bag received his M.Tech degree from West Bengal University of Technology, West Bengal, India. He received Ph.D. degree in Engineering from the Department of Engineering and Technological Studies, University of Kalyani in the year 2021. He is currently working as an Assistant Professor at the Department of Electronics and Communication Engineering, Haldia Institute of Technology. His research interests include microstrip antenna design for wireless communication systems and FSS design.



Sushanta Sarkar received his M.Tech degree from Kalyani Govt. Engineering College in the year 2010. He received Ph.D. degree in Engineering from the Department of Engineering and Technological Studies, University of Kalyani in the year 2015. He is currently working in the rank of Assistant Professor at the Department of Engineering and Technological Studies, University of Kalyani.



Partha Pratim Sarkar received his M.E. degree from Jadavpur University in the year 1994. He received Ph.D. degree in Engineering from Jadavpur University in the year 2002. He is currently working in the rank of Professor at the Department of Engineering and Technological Studies, University of Kalyani. His areas of research include microstrip antenna, microstrip filter, frequency selective surfaces, and artificial neural network.

https://doi.org/10.1017/S175907872510264X Published online by Cambridge University Press